HHS Public Access

Author manuscript

Neurosci Lett. Author manuscript; available in PMC 2018 August 02.

Published in final edited form as:

Neurosci Lett. 2015 September 14; 604: 183–187. doi:10.1016/j.neulet.2015.07.024.

Manipulating neuronal activity in the mouse brain with ultrasound: A comparison with optogenetic activation of the cerebral cortex

Michele E. Moore, **John M. Loft**, **William C. Clegern**, and **Jonathan P. Wisor***

College of Medical Sciences and Department of Integrative Physiology and Neuroscience, Washington State University, Spokane

Abstract

Low-intensity focused ultrasound induces neuronal activation via mechanisms that remain to be elucidated. We recorded local field potential fluctuations in the motor cortex in response to ultrasound stimulation of the somatosensory barrel cortex, comparing them to those recorded in response to optogenetic stimulation of interneurons and pyramidal neurons of the somatosensory cortex in the same animals. Comparison of the waveform produced by ultrasound stimulation to those produced by optogenetic stimulation revealed similarities between ultrasound-induced responses and optogenetically-induced responses to pyramidal cell stimulation, but not interneuron stimulation, which may indicate that ultrasound stimulation is mediated by excitation of cerebral cortical pyramidal neurons. Comparison of *post mortem* evoked responses to responses in living tissue confirmed the necessity for excitable tissue in the evoked response. Collectively, these experiments demonstrate an excitation-dependent response to low-frequency transdural ultrasound stimulation of cerebral cortical neuronal activity.

Keywords

transdural pulsed ultrasound; cerebral cortex; pyramidal neurons; optogenetics; interneurons; local field potentials

INTRODUCTION

Direct excitation of neuronal activity in the cerebral cortex has applications in both experimental and therapeutic contexts. Optogenetic techniques allow for direct manipulation of ion concentration gradients across the cell membrane with millisecond precision [3]. While optogenetic methods are applicable in experimental contexts, non-invasive methods of manipulating neuronal activity are preferable for applications in humans. Ultrasound stimulation may be useful for non-invasive stimulation of brain circuits in rodents [6, 12, 13]

*Corresponding author: (Jonathan.Wisor@wsu.edu), PO Box 1495, Washington State University, Spokane, Spokane, WA 99210-1495, phone: (509)358-7577, FAX: (509)358-7661.

and humans [7–9]. Ultrasound waves might generate ion fluxes by disrupting the integrity of otherwise ion-impermeant lipid bilayers in the brain [14].

The current report adapted methods and procedures of prior published work [12, 13] to produce a system in which head-to-head comparison of optogenetic and ultrasound manipulations of rodent cerebral cortical neurons was performed. The immediate goal was to test the hypothesis that a discrete circuit in the cerebral cortex is electrophysiologically responsive, at the level of the LFP, to non-invasive low frequency ultrasound stimulation. Accordingly, stimuli were delivered to the mouse primary somatosensory barrel cortex and evoked responses were measured in the primary motor cortex that receives direct monosynaptic inputs from the primary somatosensory barrel cortex [2].

MATERIALS AND METHODS

2.1 Regulatory compliance

Experiments were performed in accordance with Washington State University Institutional Animal Care and Use Committee-approved protocols and National Institutes of Health guidelines [5].

2.2 Surgical procedures

Surgical procedures were performed under sterile conditions. Anesthesia was administered in medical grade oxygen via an IMPAC Multi Patient system from Vet Equip Inc. 5% isoflurane was used for induction and 2.5% to maintain the animal during surgery. Stimuli were applied under 1.5% isoflurane. The stereotaxic apparatus was kept on a heating pad at 37°C to maintain body temperature. After clearance and sterilization of the skull, bregma was located by visual inspection. Holes were placed (using a 0.5 mm ball burr bit) relative to bregma at 0.86 mm anterior/1.5 mm left (left motor); 2 mm anterior/1.5 mm left (left frontal); 1 mm posterior/1.5 mm right (right parietal); 3 mm posterior/1.5 mm right (right occipital). A craniotomy approximately 3 × 3 mm square was performed on the region surrounding the left somatosensory barrel cortex (1.7 mm posterior/2.5 mm left relative to bregma; a source of direct neuronal connections to left motor cortex [2]) using a high-speed dental drill with a 0.5 mm ball burr bit, without disturbing the dura mater. The craniotomy was necessary for delivery of light onto the cerebral cortex for optogenetic stimulation. The same site was used for ultrasound and optogenetic stimulation, stimulation was transdural, not transcranial *per se*. A tungsten electrode was constructed from PFA coated tungsten wire (A-M Systems; Sequim, WA; Catalog No. 797000, 0.008″ bare diameter, AWG 32). A 90-degree bend was placed in the wire, leaving a length of 2.0 mm distal to the bend, which rested on the skull, for insertion of the electrode into the brain. This electrode was placed in the left motor cortex via the hole drilled there. Stainless steel EEG screws (1/16 inch diameter) were placed in the left frontal hole (reference for motor lead), right parietal hole (cable ground) and right occipital hole (body ground affixed to the surgical table with Alpha Wire, 2840/7, 32 AWG, DigiKey). Ortho-Jet Acrylic Resin, a fast curing, 2-part orthodontic acrylic resin, was used to secure electrodes in place.

Grounding was performed immediately prior to the commencement of recording. A wire was attached to the stereotaxic device and connected directly to the surgical table. The entire stereotaxic plate was covered with a cube shaped Faraday cage (copper wire mesh secured to a PVC frame; approximately 0.5 m × 0.5 m × 0.5 m) to eliminate electrical noise. The cage was also connected to the surgical table via a grounding wire and alligator clip. The surgical table was grounded to the 'earth' ground present in the electrical outlet in the wall via an additional grounding wire. All other wires were soldered to an electrode montage (Mill-Max Manufacturing Corp. from Digi-Key, part #ED8250-ND), which connected to an 8-channel miniature preamplifier (Multichannel Systems, Inc; Reutlingen, Germany; MPA81).

2.3 Stimulation apparatus and stimulus timing

A TTL trigger from a stimulus generator (Multichannel Systems STG4002 TTL generator, programmed with *MC_Stimulus II* software) served to trigger, via 5 V signal, both the optogenetic (LED) and ultrasound power sources. For optogenetic stimulation, the LED was programmed to be on continuously for 10 ms of every 142 ms (7 Hz; 7% duty cycle) as a function of this TTL input square pulsed wave. The optogenetic stimulation system consisted of a TTL stimulus generator (STG4002), an LED, a power supply, and a fiber optic cable. An LED driver (Doric Lenses, product # D480-1003; LED_DRV_1CH, version 2012 with an independent power cord) was the power source for the LED light source. Procedures for optogenetic stimulation are otherwise as described elsewhere [4, 15]. Ultrasound stimulation procedures were modeled on [13] for the assembly and programming of the waveform generators and the RF amplifier used to power the ultrasound transducer. For ultrasound stimulation, signal was generated by two Agilent Waveform Generators (33220A; 20 MHz) triggered in serial by the TTL pulse (Figure 1). The TTL generator square pulsed wave triggered waveform generator 1 to undergo a square wave train of 10 ms duration. During each 10 ms stimulus train, waveform generator 1 produced twenty 5 V_{pp} square pulsed waves (each of 0.5 ms duration) with a 50% duty cycle, yielding a square pulsed wave repetition frequency of 2.0 kHz. At the onset of each of these 20 square pulsed waves, waveform generator 2 triggered the transducer to undergo 75 acoustic cycles at an acoustic frequency of 350 kHz (yielding an ultrasound event duration of approximately 0.214 ms). The duty cycle for these 350 kHz ultrasound events was thus (0.214 ms)/(0.5 ms)*100%= 42.8%.

We used a gas matrix piezoelectric-based contact/immersion transducer from the Ultran Group (State College, PA, USA; model # GS350-D19). This planar transducer's active diameter was 19 mm and its nominal frequency was 350 kHz. Although acoustic intensity was not measured in our experimental apparatus, acoustic intensity of this transducer used in the configuration applied here is reported as 0.07–0.23 W/cm^2 [12, 13]. A polyethylene column (length 4 mm) was coupled to the transducer via a tapered transducer cap. The internal diameter of this column tapered from 3 mm at the end receiving ultrasound input to 2 mm at the end contacting the animal. The transducer/coupler interface and coupler column were filled with ultrasound gel. The ultrasound transducer was placed into a circular holder accessory and attached to the stereotaxic device. The stereotaxic arm was used to position the end of the coupler column against the animal's skull around the rim of the craniotomy. The stereotaxic arm was lowered until the surrounding skull was seen to flex.

2.4 Recording optogenetic and ultrasound electrophysiological responses

Data were collected by Multichannel Systems MC_Rack software version 4.4.8 with settings of amplifier gain 1000, input voltage range = +/− 819.2 mV, and sampling frequency 5000 Hz. The TTL signal from the STG4002 TTL generator was collected by the software as an additional channel. Data were processed with a Butterworth 2nd order filter with a high pass of 0.5 Hz. Data files were recorded in the custom format of Multichannel Systems. MC_DataTool software was used to convert this file to a raw binary file for data analysis in the MATLAB programming environment. To account for drift in the signal, data were subjected to normalization, first by subtracting the mean of all sampled values across the recording from each individual sampled value in the recording. Next, the data were subjected to a smoothing algorithm, in which the mean of the potential across a 3-sec window centered on each data point was subtracted from the value at that data point. Use of the 3-second window served to minimize the effect of evoked potential changes, relative to baseline potential on the normalization of values, as it included data from > 20 stimulus on-off cycles. A single vector consisting of 15,000 data points (3 seconds of data) was generated from these transformed potential values by averaging values across 3-second segments of data centered on every TTL-triggered stimulus onset in the file. For the purpose of data visualization (though not data analysis) this averaged curve for the recording was subjected to a 60-Hz bandstop elliptic filter. An output routine for exporting the average response of all stimuli in each recording into a spreadsheet allowed for statistical analysis across the entire data set of animals. Statistica 9.0 (StatSoft; Tulsa, OK) was used for descriptive and inferential statistics. SigmaPlot (Systat Software, Inc. San Jose, CA) was used to generate graphs.

2.5 Experiment 1: Evoked potentials in distinct optogenetic models

Experiment 1 used two transgenic lines of mice expressing ChR2 in distinct cell types of the cerebral cortex. In Thy1-ChR2 transgenic mice (JAX strain #7612), the Thy1 promoter drives expression of ChR2 in cortical pyramidal cells [1]. Male mice heterozygous for this transgene (n=4), used in these experiments, were generated by crossing homozygous transgenic mice from the JAX 7612 strain with transgene-negative mice of the CD-1 strain. nNOS-ChR2 transgenic mice were generated by crossing two lines of mice available through JAXMice.org. In B6;129S- Nos1tm1.1(cre/ERT2)Zjh/J; JAX stock # 14541, Cre recombinase expression is driven by the nNOS promoter. In mice of the B6;129-Gt(ROSA)26Sortm1(CAG-COP4*E123T*H134R,-tdTomato)Gfng/J line JAX stock # 17455, a loxP-silenced genetic construct containing ChR2 is present in the *rosa26* locus. Crossing of these two strains and treating resulting offspring (heterozygous for both constructs) with tamoxifen (20 mg/mL by oral gavage) daily for three days activates the estrogen receptor (ER)-dependent Cre construct, causing Cre-dependent unsilencing of the ChR2 transgene in nNOS positive cells [11]. n=5 nNOS-ChR2 male mice were subjected to experimentation. Doubly-heterozygous litter mate male mice (n=5) treated with corn oil via oral gavage served as optogenetically-unresponsive (referred to hereafter as non-ChR2) controls. Histological processing of cortical tissue demonstrated transgene expression in nNOS-positive cells of the cerebral cortex only in tamoxifen-treated mice (data not shown).

Each mouse was subjected to a ten-minute recording of ultrasound stimulation and a ten-minute recording of optogenetic stimulation. Stimulation events (10 ms stimulus trains of ultrasound stimuli or 10 ms continuous light exposure in optogenetic protocols) were delivered at 7 Hz throughout the duration of the ten-minute recordings. This stimulation frequency was chosen to minimize any possible effect of 60 Hz noise on the signal, as it is not a divisor of the 60 Hz noise band.

For statistical analysis of evoked potentials, averaged curve data were downsampled 10-fold to 500 Hz, by averaging across 10 consecutive values from the 5000 Hz signal. Statistical analyses of ultrasound and optogenetic data were performed separately. Stimulation events occurring over the ten-minute interval were divided into 2.5-minute quartiles (n=1050 stimulation events per quartile). Within each quartile of recording time, averaged curves (downsampled to 500 Hz) were generated by averaging the data from each of 1050 100-ms windows beginning 20 ms before the onset of each stimulation event. As a control, averaged curves were generated by averaging the data from each of 1050 randomly-timed segments of data from the same recording. In order to determine whether the genotype affected the evoked response, these averaged curves from all stimulus events in the first quartile of recording time were subjected to repeated measures ANOVA with genotype as a between-subjects variable, data trace (random vs. evoked) as a within-subjects variable and time relative to stimulation event onset as a within-subjects variable. In order to determine whether the evoked response to either ultrasound or optogenetic stimuli attenuated over time, data were subjected to repeated measures ANOVA with quartile, data trace (random vs. evoked) and time relative to stimulation event onset as within-subjects variables. Where this ANOVA indicated a significant effect of quartile (optogenetic stimulation of Thy1-ChR2 mice only), an additional analysis was performed to quantify the effect of quartile on amplitude of evoked events. Within each quartile, the trough and peak values were measured at 5 and 20 msec, respectively, relative to stimulus offset in the averaged evoked curves. Maximum values and minimum values were then subjected to one-way repeated measures ANOVA with quartile as a within-subjects factor.

2.6 Experiment 2: Evoked potentials in living vs. post mortem conditions

This experiment used eight male Thy1-ChR2 transgenic mice. Mice were subjected to electrophysiological recordings during 10-minute applications of 10 ms optogenetic stimulation events and 10 ms ultrasound stimulation events as in experiment 1. They were then euthanized by cervical dislocation and anesthesia was terminated. Animals were kept on heating pads *post mortem* to maintain temperature. Five minutes after euthanasia, the optogenetic and ultrasound stimulation protocols were repeated in identical fashion as in live animals immediately prior to euthanasia.

Data processing was performed as in experiment 1, except that data represent averaged curves from the entire 10-minute recording. Negative deflections were defined as the interval between each downward zero cross and the subsequent upward zero cross. Positive deflections were defined as the interval between each upward zero cross and the subsequent downward zero cross. Event duration was the time lapsed from the zero cross defining

deflection onset and the zero cross defining deflection offset. AUC was calculated by summation of all electrical potential values across the duration of that deflection.

3. RESULTS

3.1 Comparison of ultrasound-evoked potentials to optogenetically-evoked potentials

Application of blue light pulses of 10 ms to the somatosensory barrel cortex of transgenic mice expressing ChR2 in pyramidal neurons (Thy1-ChR2) or nNOS-positive cells (nNOS-ChR2) triggered distinct fluctuations in LFP in the motor cortex. Stimulus application caused a negative deflection indicative of depolarization at the cellular level in Thy1-ChR2 (Figure 2A) mice and, by contrast, a positive deflection indicative of hyperpolarization at the cellular level in nNOS-ChR2 transgenic mice (Figure 2B). In both transgenic lines, these responses were followed by reversal of the potential at stimulus offset (time 10 ms). The optogenetic response was dependent on ChR2 transgene expression: non-expressing mice subjected to optogenetic stimulation did not exhibit significant evoked responses (non-ChR2 controls; Figure 2B, inset). The evoked response to 10 ms ultrasound stimulation was not affected by genotype or genotype X time interaction ($P>0.90$), and consequently evoked responses to ultrasound (Figure 2C) were collapsed across genotypes for display and statistics. The evoked response to 10 ms ultrasound stimulation was, similar to optogenetic activation of pyramidal cells, characterized by a negative deflection during stimulation, followed by reversal to a positive deflection. The amplitudes of the ultrasound-evoked responses were 10-fold (negative deflection) to 20-fold (positive deflection) smaller in amplitude than those evoked by optogenetic stimulation of pyramidal cells.

The amplitude of optogenetically-evoked responses to pyramidal cell stimulation in Thy1-ChR2 mice changed as a function of time across an interval of 10 minutes of 7 Hz stimulation when data were measured in quartiles of 1050 stimuli (Figure 3A; $F_{147,441}=1.80$; $P<0.001$). Peak negative ($F_{3,9}=6.48$; $P=0.013$, repeated measures ANOVA, main effect of quartile) and positive values ($F_{3,9}=6.05$; $P=0.015$), when normalized to their magnitude in the first quartile of stimulation in Thy1-ChR2 mice (Figure 3A, inset) exhibited a significant effect of quartile. In the fourth quartile of stimulation (7.5–10 minutes), the magnitude of the immediate negative deflection was significantly attenuated to 72% of the response in the first quartile (0–2.5 minutes); the magnitude of the subsequent positive deflection was significantly attenuated to 84% of the response in the first quartile. Evoked responses to optogenetic stimulation of nNOS-ChR2 mice ($P=0.34$) and ultrasound stimulation across all genotypes ($P=0.32$) did not differ across the quartiles of the 10-minute continuous stimulation session.

3.2 Comparison of responses in live vs. *post mortem* animals

The durations and AUC detected from the positive and negative deflections were significantly affected by physiological state (alive vs. *post mortem*) for optogenetic stimulation ($F_{1,20} \geq 8$ for main effect of state on duration of negative deflection, AUC of negative deflection, duration of positive deflection and AUC of positive deflection; all $P < 0.01$) and ultrasound stimulation ($F_{1,20} \geq 4$ for main effect of state on duration of negative deflection, AUC of negative deflection, duration of positive deflection and AUC of positive

deflection; all $P < 0.05$). The durations and AUC for both the negative and subsequent positive deflections were reduced in *post mortem* tissues relative to living tissues (Figure 4), indicating a requirement for living tissue in the evoked response.

DISCUSSION

Optogenetic targeting of distinct populations, the pyramidal population and the nNOS-positive GABAergic population, yielded distinct responses. Since the stimulus was delivered to the somatosensory cortex and the response measured in its monosynaptic target (the motor cortex), the negative deflection in Thy1-ChR2 mice likely reflects activation of the post-synaptic targets of the neurons directly stimulated in the somatosensory cortex. The inverted response in the nNOS-ChR2 mice relative to the Thy1-ChR2 mice is to be expected, as these long-projecting GABAergic cells [10] inhibit their post-synaptic targets.

The temporal profile of the evoked response to ultrasound stimulation, a negative deflection indicative of depolarization, was similar to that of optogenetic stimulation of pyramidal cells, which is known to result in their depolarization [16]. Thus, the response to ultrasound appears to be depolarization. The 10- to 20-fold difference in magnitude between these two stimulation modes likely indicates differences in the number of cells recruited. However, since the acoustic intensity and acoustic field were not measured in the current study, it is not possible to determine the spatial extent of neurons activated by ultrasound.

Ultrasound stimulation additionally differed from optogenetic stimulation of pyramidal cells in that the response to ultrasound did not attenuate, whereas the response to optogenetic stimulation of pyramidal cells (but not the response to nNOS cell stimulation) did attenuate modestly over time. The reason for attenuation of the response to stimulation in the Thy1-ChR2 mice is uncertain. As the response to optogenetic stimulation in the Thy1-ChR2 mice was of much greater magnitude than the modest responses to nNOS-ChR2 and ultrasound stimuli, it may have been more demanding metabolically and therefore more prone to attenuate over time.

To the extent that non-physiological, electromechanical fluctuations (including possibly electrical noise) occurred in the cerebral cortex *post mortem*, they were significantly smaller than those occurring in live tissue, as indicated by significant effect of *post mortem* status on the duration and AUC values for the immediate negative and subsequent positive deflections of field potential.

Acknowledgments

We thank Michelle A. Schmidt for generating and managing the colony of animal subjects used in these experiments. Research supported by RO1NS078498 and RO3NS082973.

ABBREVIATIONS

ANOVA	analysis of variance
AUC	area under the curve

ChR2	Channelrhodopsin2
LFP	local field potential
PFA	perfluoroalkoxy alkane
TTL	transistor-transistor logic
LED	light-emitting diode
RF	radio frequency

References

1. Arenkiel BR, Peca J, Davison IG, Feliciano C, Deisseroth K, Augustine GJ, Ehlers MD, Feng G. In vivo light-induced activation of neural circuitry in transgenic mice expressing channelrhodopsin-2. Neuron. 2007; 54:205–218. [PubMed: 17442243]
2. Aronoff R, Matyas F, Mateo C, Ciron C, Schneider B, Petersen CC. Long-range connectivity of mouse primary somatosensory barrel cortex. Eur J Neurosci. 2010; 31:2221–2233. [PubMed: 20550566]
3. Boyden ES, Zhang F, Bamberg E, Nagel G, Deisseroth K. Millisecond-timescale, genetically targeted optical control of neural activity. Nat Neurosci. 2005; 8:1263–1268. [PubMed: 16116447]
4. Clegern WC, Moore ME, Schmidt MA, Wisor J. Simultaneous electroencephalography, real-time measurement of lactate concentration and optogenetic manipulation of neuronal activity in the rodent cerebral cortex. J Vis Exp. 2012:e4328. [PubMed: 23271428]
5. N.R.C. Institute of Laboratory Animal ResourcesGuide for Care and Use of Laboratory AnimalsNational Academy Press; Washington, DC: 1996
6. King RL, Brown JR, Newsome WT, Pauly KB. Effective parameters for ultrasound-induced in vivo neurostimulation. Ultrasound in medicine & biology. 2013; 39:312–331. [PubMed: 23219040]
7. Lee W, Kim H, Jung Y, Song IU, Chung YA, Yoo SS. Image-guided transcranial focused ultrasound stimulates human primary somatosensory cortex. Scientific reports. 2015; 5:8743. [PubMed: 25735418]
8. Legon W, Sato TF, Opitz A, Mueller J, Barbour A, Williams A, Tyler WJ. Transcranial focused ultrasound modulates the activity of primary somatosensory cortex in humans. Nat Neurosci. 2014; 17:322–329. [PubMed: 24413698]
9. Mueller J, Legon W, Opitz A, Sato TF, Tyler WJ. Transcranial focused ultrasound modulates intrinsic and evoked EEG dynamics. Brain Stimul. 2014; 7:900–908. [PubMed: 25265863]
10. Perrenoud Q, Geoffroy H, Gauthier B, Rancillac A, Alfonsi F, Kessaris N, Rossier J, Vitalis T, Gallopin T. Characterization of Type I and Type II nNOS-Expressing Interneurons in the Barrel Cortex of Mouse. Front Neural Circuits. 2012; 6:36. [PubMed: 22754499]
11. Taniguchi H, He M, Wu P, Kim S, Paik R, Sugino K, Kvitsiani D, Fu Y, Lu J, Lin Y, Miyoshi G, Shima Y, Fishell G, Nelson SB, Huang ZJ. A resource of Cre driver lines for genetic targeting of GABAergic neurons in cerebral cortex. Neuron. 2011; 71:995–1013. [PubMed: 21943598]
12. Tufail Y, Matyushov A, Baldwin N, Tauchmann ML, Georges J, Yoshihiro A, Tillery SI, Tyler WJ. Transcranial Pulsed Ultrasound Stimulates Intact Brain Circuits. Neuron. 2010; 66:681–694. [PubMed: 20547127]
13. Tufail Y, Yoshihiro A, Pati S, Li MM, Tyler WJ. Ultrasonic neuromodulation by brain stimulation with transcranial ultrasound. Nat Protoc. 2011; 6:1453–1470. [PubMed: 21886108]
14. Tyler WJ. Noninvasive neuromodulation with ultrasound? A continuum mechanics hypothesis. Neuroscientist. 2011; 17:25–36. [PubMed: 20103504]
15. Wisor JP, Rempe MJ, Schmidt MA, Moore ME, Clegern WC. Sleep slow-wave activity regulates cerebral glycolytic metabolism. Cereb Cortex. 2012; 23:1978–1987. [PubMed: 22767634]

16. Zhang F, Wang LP, Brauner M, Liewald JF, Kay K, Watzke N, Wood PG, Bamberg E, Nagel G, Gottschalk A, Deisseroth K. Multimodal fast optical interrogation of neural circuitry. Nature. 2007; 446:633–639. [PubMed: 17410168]

HIGHLIGHTS

- optogenetic stimulation of pyramidal cells and interneurons evoke distinct responses
- low-intensity ultrasound-evoked responses resemble pyramidal cell-evoked responses
- ultrasound-evoked responses do not attenuate over 10-minute stimulus intervals

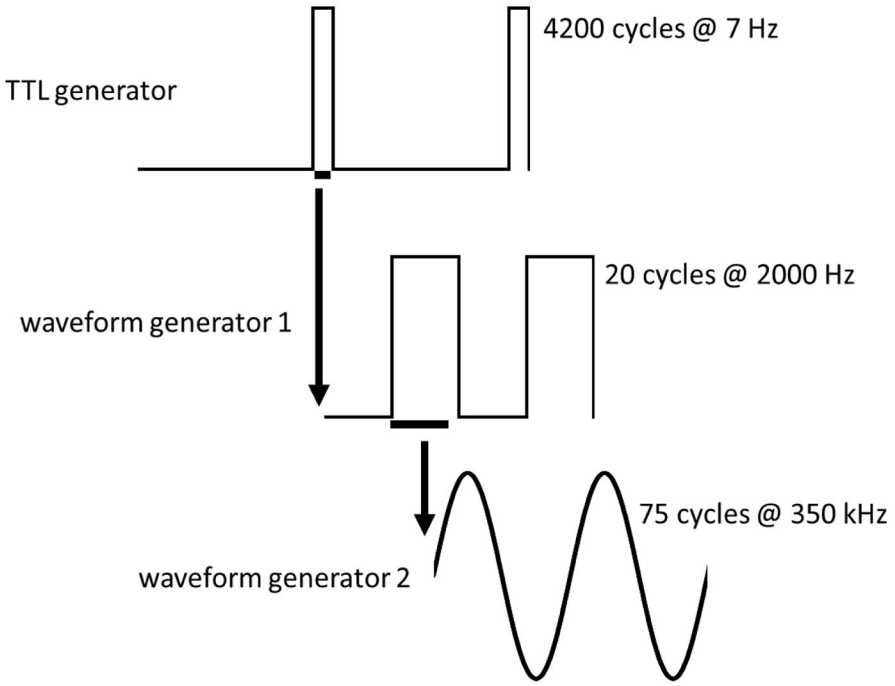

Figure 1.

Ultrasound stimulus timing. Two complete cycles of signal from each generator are shown. A TTL generator produced a 5 V pulse of 10 ms duration at a frequency of 7 Hz. Waveform generator 1 then produced 20 5 V pulses of 0.5 ms duration at a frequency of 2000 Hz. Waveform generator 2 then underwent 75 350 kHz sinusoid waves which were transduced into acoustic waves.

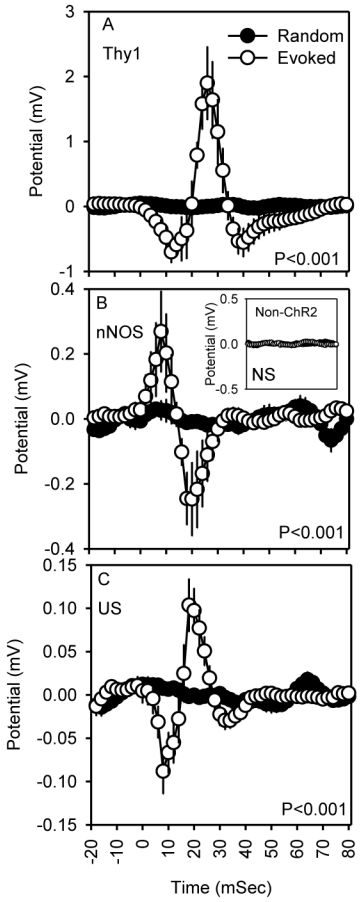

Figure 2.

Evoked responses (mean ± SEM) to optogenetic stimuli in Thy1-ChR2 transgenic (A; n=4), optogenetic stimuli in nNOS-ChR2 transgenic (B; n=5) and ultrasound stimuli across all genotypes of mice studied (C; n=14). Time zero is the time of stimulus onset. P values are the effect of time on potential. Inset in B shows equivalent optogenetic stimulation data from mice not expressing ChR2 (n=5).

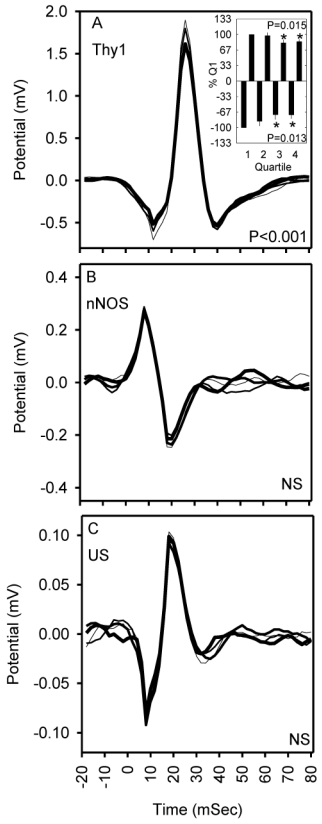

Figure 3.

Effects of repeated stimulation on evoked responses to optogenetic stimuli in Thy1-ChR2 transgenic mice expressing ChR2 in cortical pyramidal cells (A), optogenetic stimuli in nNOS-ChR2 transgenic mice expressing ChR2 in cortical interneurons (B) and ultrasound stimuli across all genotypes of mice studied (C). Sequential 2.5-min quartiles of stimulation in each graph are represented by curves of increasing thickness. P values refer to quartile X time interaction. Inset in A shows the magnitude of the peak negative (5 ms after stimulus offset) and positive (20 ms after stimulus offset) deflections across quartiles as a percentage of first quartile values. P values in inset refer to effect of quartile on response magnitude. *, Fisher's LSD indicated that the response was significantly attenuated in quartiles 3 and 4 relative to 1.

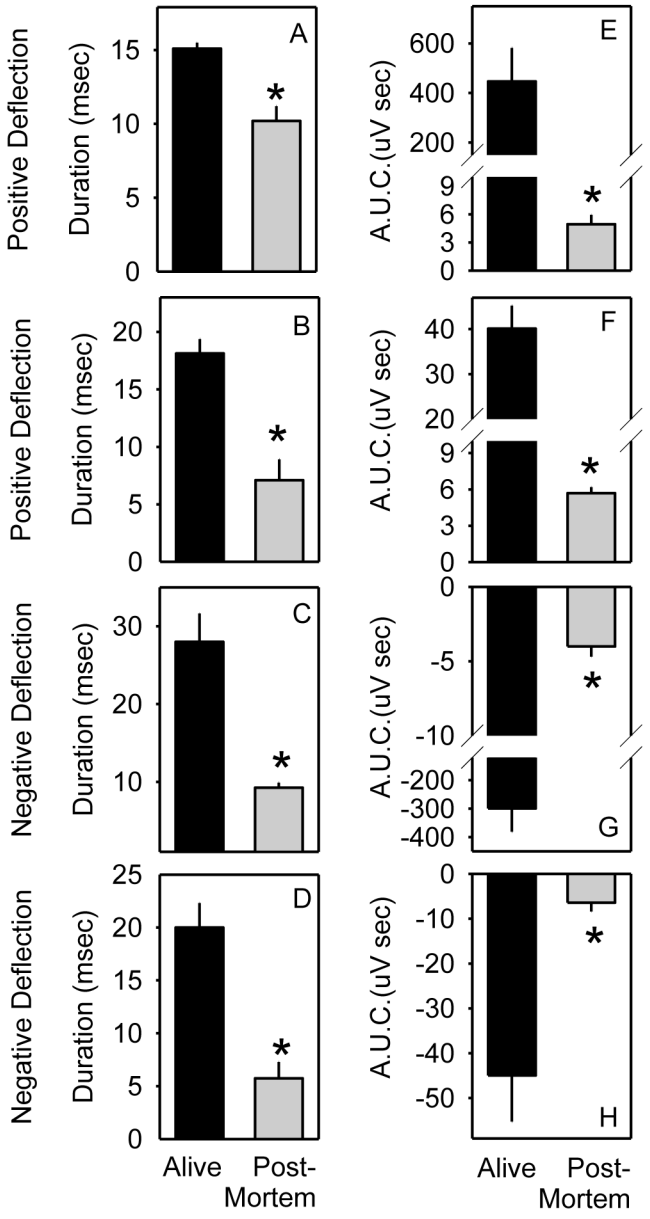

Figure 4.

Evoked response parameters are dependent on living tissue. A–D, duration of positive and negative deflections during evoked responses to optogenetic (A,C) and ultrasound stimuli (B,D). E–H area under the curve (A.U.C.) of positive and negative deflections during evoked responses to optogenetic (E,G) and ultrasound stimuli (F,H). *, Fisher's LSD indicated that the response was significantly attenuated when measured *post mortem* (gray bars) relative to in living tissue (black bars).